Paper offer 06B-183 (B20)

Inverse Finite Element Characterization of Soft Tissues Using Impact Experiments and Taguchi Methods

Karthikeyan Balaraman, Sudipto Mukherjee, Anoop Chawla
Department of Mechanical Engineering, Indian Institute of Technology Delhi

Rajesh Malhotra
Department of orthopaedics, All India Institute of Medical Sciences

ABSTRACT

The objective of this study is to establish a methodology to identify the dynamic properties of soft tissues. Nineteen in vitro impact tests are performed on human muscles at three average strain rates ranging from 136/s to 262/s. Muscle tissues are compressed uniaxially up to 50% strain level. Subsequently, finite element simulations replicating the experimental conditions are executed using the PAM-CRASH^{TM}, explicit finite element solver. The material properties of the muscles, modelled as linear isotropic viscoelastic material, are identified using inverse finite element mapping of test data using Taguchi methods. Engineering stress - engineering strain curves from experimental data and finite element models are computed and compared during identification of material properties at the above mentioned strain rates. Response of finite element models, with extracted material properties, falls within experimental corridors indicating the validation of the methodology adopted.

INTRODUCTION

Finite element human body models have significant applications in pedestrian and occupant safety in automobile crashes (Maeno et al. 2001, Oshita et al. 2002). Existing models lack in predicting the soft tissue characteristics, when subjected to dynamic loadings due to unavailability of strain rate dependent material properties (Iwamoto et al. 2003). Testing procedures using quasi-static compression experiments (Miller et al. 1997, Miller Young et al. 2002), ramp tests (Bosboom et al. 2001), aspiration experiments (Kauer et al. 2002) and indentation tests (Durand-Revillie et al. 2004, Delalleau et al. 2005, Erdemir et al. 2005) are widely reported to characterize the soft tissues at lower strain rates, less than 100/s using inverse characterization techniques. Most of these studies use nonlinear optimization algorithms like Levenberg-Marquardt method (Kauer et al. 2002, Moulton et al. 1995). These gradient-based methods involve complex derivatives in constitutive equations, difficult to calculate for complex material models. Material characterization of soft tissues under impact loads for strain rates ranging from 100/s to 500/s is of interest in biomechanical arena to simulate the human injuries in automobile crashes. Inverse characterization studies for identifying the soft tissue material properties satisfying these conditions are limited. To address this issue a procedure to identify the dynamic material properties using Taguchi methods is presented in this study by comparing the experimental and finite element stress-strain response and minimizing the error between them for optimal fit.

TAGUCHI METHODS

Taguchi methods, well known for its industrial applications to identify sensitive parameters for a given target, find fewer applications in biomechanics, particularly on material property identification. Taguchi methods use fractional factorial design in the form of an orthogonal array to identify the design parameters like material properties for achieving the target response, optimal fit of experimental-simulation stress-strain response. Taguchi methods can be utilized to arrive at the best parameters for the optimum design configuration with least number of analytical investigations. By identifying the sensitivity of the design parameters, a systematic mapping can be performed for faster convergence. A detailed description of this method can be found in Roy 1990, Bagchi 1993. Dar et al. 2002 presented the application of statistical methods, involving probabilistic analysis and fractional factorial design using Taguchi methods, in finite element analysis and demonstrated the input parameter identification process in a simple cantilever beam problem. The advantage of Taguchi methods in reducing the experimental effort by identifying and operating with the sensitive input parameters is emphasized. Ng et al. (2004) conducted a fractional factorial analysis on the finite element model of the cervical vertebra to analyze the influence of spinal components on the internal stresses and external biomechanical responses under compression, anterior shear and posterior shear.

METHODS

The scheme for identifying the dynamic material properties of soft tissues using inverse finite element characterization is shown in Figure 1.

IMPACT EXPERIMENTS

In the present study the experimental data used to characterize the soft tissues is acquired from impact experiments. A total of 19 successful tests are performed for uniaxial compressive-impact loading at three different strain rates ranging from 136/s to 262/s. This study does not consider the demographics, etiology and anatomy selected and also its dependency for exercising the muscles as it falls beyond its scope. This study focuses on establishing the methodology to identify the material properties of soft tissues rather than predicting the dependency of impact response on those parameters.

Specimen preparation

Human extremity muscles harvested from three living human subjects are obtained from All India of Medical Sciences (AIIMS) with their prior approval to this study. All the obtained tissues are considered as healthy tissues when removed during medical surgery without physical damage. These tissues are not physically loaded at any time till conducting actual tests. The tissues extracted from the human subjects are grouped and identified as Human1 (H1), Human2 (H2) and Human3 (H3) in this entire study, representing the individuals. The regional location of the tissue and the number of samples tested is indicated in Table 1. Muscles from lower extremity region (thigh) are obtained from the subjects H1 and H2; muscles from the upper extremity region (shoulder) are obtained from the subject H3. All the specimens collected after the surgery are wrapped in polythene sheet and frozen at -20 deg. C for two weeks (Van Ee et al. 1998, 2000). Three hours before testing, specimens are thawed at room temperature 20 deg. C. Specimens has not been preconditioned before conducting the actual tests. Fascia layer is removed from the tissue. Measures are taken to prevent the dehydration of the tissue during testing.

Table 1. Subject Identification

Subject Identification	Muscle region in the human body	Number of specimens tested
H1	Lower extremity	3
H2	Lower extremity	8
H3	Upper extremity	21

Cubical specimens are prepared using surgical scalpel with a uniform square cross sectional area of 14 x 14 mm, approximately. The dimensions recorded tend to have deviation from 0.25 to 0.5 mm as measurement error. The sample height is measured in the direction perpendicular to fiber orientation in anterior-posterior direction using high-speed photography is listed in Table 2 for successful tests. A total of thirty-two specimens are prepared from the muscles harvested from three human subjects. All the tests are performed in unconfined condition.

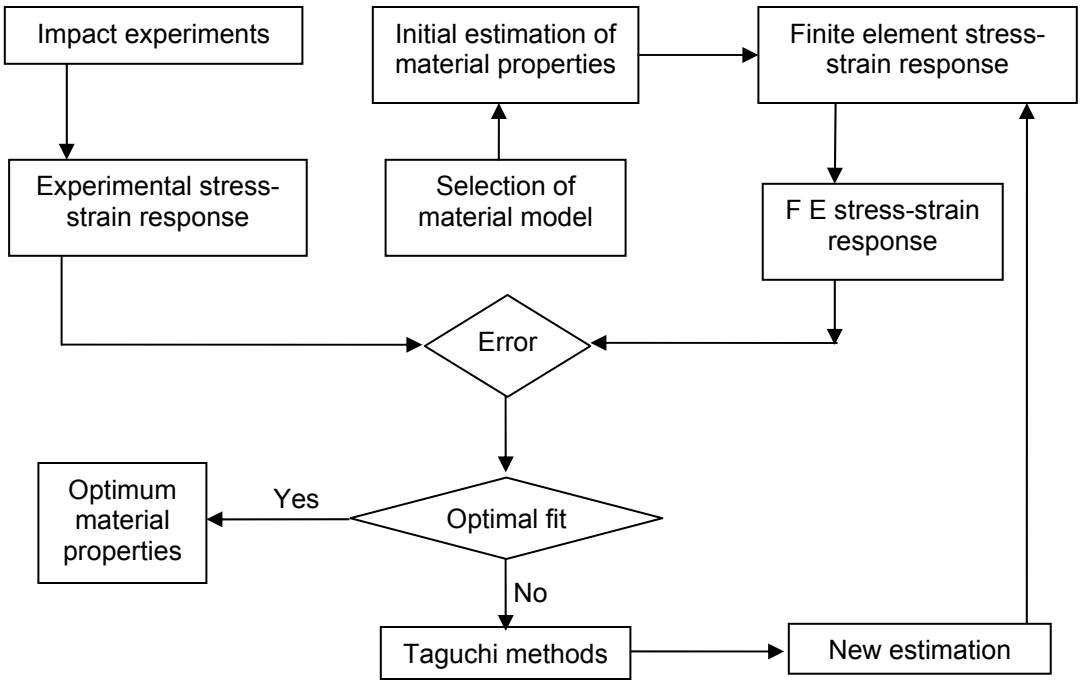

Figure 1. Schematic diagram of parameter estimation procedure

Table 2. Successful tests and individual strain rate along with the measured initial velocity

Subject ID – Test ID	Specimen height (mm)	Initial velocity (m/s)	Strain rate (s^{-1})	Strain rate group (Mean +/- SD, n)
H2-T07	9.5	1.23	129	Lower strain rate (136+/19.94, n=7)
H3-T01	8.5	1.13	133	
H3-T03	11.0	1.18	107	
H3-T04	9.0	1.20	134	
H3-T10	9.5	1.21	127	
H3-T11	7.5	1.22	163	
H3-T12	7.5	1.22	162	
H3-T05	10.5	1.80	172	Medium strain rate (183+/-6.80, n=5)
H3-T06	9.0	1.72	191	
H3-T07	9.0	1.66	184	
H3-T15	10.0	1.83	183	
H3-T17	10.5	1.92	183	
H1-T03	8.5	2.30	271	Higher strain rate (262+/- 31.63, n=7)
H2-T05	8.0	2.27	284	
H2-T06	7.5	2.18	291	
H2-T08	10.0	2.07	207	
H3-T08	8.5	2.30	271	
H3-T09	8.5	2.40	282	
H3-T19	10.5	2.40	229	

Experimental set-up

A custom made uniaxial impact testing machine developed by Indian Institute of Technology Delhi, is used to test the specimens under impact loading (Figure 2). Repeatability of the impact test set-up has been established and presented in our previous work using rubber and goat soft tissues (Karthikeyan et al., 2005). The test set-up consists of a spring-loaded launcher attached with a top platen. A maximum velocity up to 8 m/s can be achieved with the existing arrangement. The mass of the impactor is 1 kg. A strain gage based force transducer (S-Type) capable of measuring both static and dynamic forces up to 1000N is mounted below the bottom platen to measure the force-time history during the test. A high-speed motion camera (REDLAKE, San Diego, CA, USA) is used to capture the event. The video is subsequently analyzed to find out the displacement of the tissue and the initial velocity of the impactor. Sensor data is acquired using an e-DAQ module (SoMat Corporation, Urbana, IL, USA), which is connected with the force transducer and trigger switch channels for acquiring the respective signals. A strain gauged cantilever beam is kept at the same level as the tissue top surface. The beam has a trigger switch, which is set to trigger both the e-DAQ and the high-speed motion camera. This triggering synchronizes the force data and displacement data from e-DAQ and high-speed motion camera respectively and helps to identify the start of the event. Specimen compression level is controlled using a rigid mechanical stopper, which constraints the motion of the top platen after the tissue gets compressed to the required distance.

Tests are performed in an unconfined condition, that is, the specimens are allowed to expand freely in the lateral direction. Unconfined tests are preferred in this study so as to reduce the number of contact surfaces and the frictional coefficients between the specimen and the constraining surfaces as it has been observed to increase the uncertainties in the experiment. Poly tetra flouro ethylene (PTFE) sheets are used as interface between the bottom platen and specimen to reduce friction. Insulation tapes were wrapped at the contacting surface of the top platen to reduce friction. In the current tests we have gone up to a measured strain of 50% in the direction of the impact.

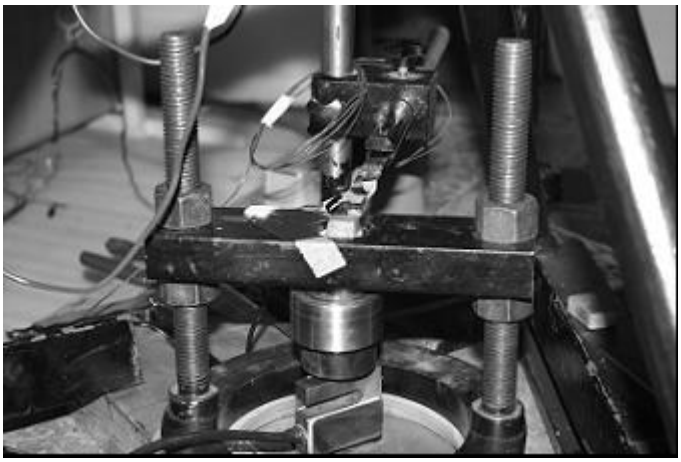

Figure 2. Impact Gun test set-up, launcher is not shown in the picture

Experimental protocol

Tests were conducted for three different strain rates at 136/s (19.9/s), 183/s (6.8/s) and 262/s (31.3/s) representing the mean (standard deviation) values. The tissue subjected to different strain rates are grouped according to the tests conducted at similar initial velocities (1.20+/-0.03 ms, 1.79 +/-0.1 m/s, 2.27 +/-0.12). Detailed list of successful tests and its individual strain rates are given in the Table 2. Among the 32 tests conducted, 7 tests from lower strain rate, 5 tests from medium strain rate and 7 tests from higher strain rates, accounting a total of 19 successful tests. All the tests are performed for 50 % compression of specimen. Force data is acquired at the rate of 10000 samples per second. The order of static noise level in the force transducer is found to be less than 0.05 N at the time of experiments. Pre-filtering and post-filtering are not preformed at any time on the data, as there was no

considerable noise in the acquired signal. High-speed motion camera pictures are captured at 5000 frames per second with a resolution of 384 x 256 pixels. Data is recorded for 0.05 seconds before trigger time and 0.49 seconds after trigger.

Data analysis

Acquired force data is post processed with N-soft™ (N-Code, Sheffield, UK) data analysis package. The displacement and velocity data is measured from high-speed motion camera data by using Image express™ software. Engineering stresses reported in this study is calculated from the ratio of force measured and initial cross sectional area. Engineering strain is calculated from the ratio of displacement and initial height of the specimen. Initial velocities of the specimens are measured by taking the average of 10 velocity data points from high speed camera data before the event start time representing duration of 2 milliseconds. Strain rate is calculated as the ratio of initial velocity and initial specimen height. The strain rate was constant throughout the test with maximum variation of 10% from the mean values. During post processing the force-time data, the sample rate is reduced from 10000 samples per second to 5000 samples per second to synchronize with the deflection-time data. From the thirty-two tests conducted, thirteen test data has not been considered during post processing on account of deviations in the experimental data recorded with others.

FINITE ELEMENT ANALYSIS

A finite element model representing the experimental conditions is developed to mimic the impact test.

Model description

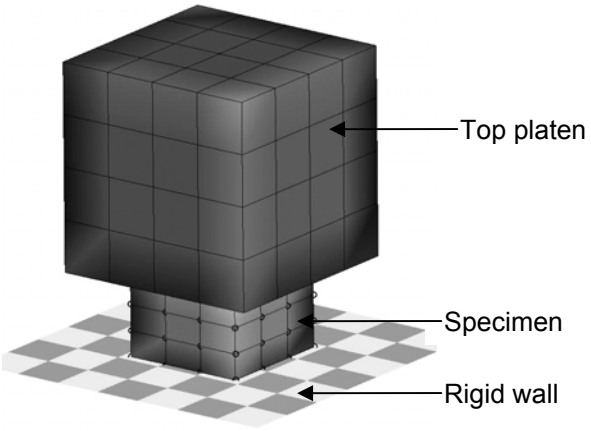

Figure 3. Finite element model of soft tissue and the top platen and rigid wall

A finite element mesh of the top platen and tissue is generated in the I-DEAS software (UGS-PLM solutions, USA) using eight-node solid elements. Finite element analysis is performed using PAM-CRASH™ (ESI group, France) (Figure 3). The model consists of 91 elements and 189 nodes. Element quality checks has been performed to identify the existence of any distorted elements and to satisfy the minimum time step criteria. A convergence study (Miller 2000) is conducted to decide upon the mesh size and number of elements. Two different mesh sizes, coarse (2mm X 2mm X 2mm) and fine mesh (1mm X 1mm X 1mm) representing length, breadth and height of the specimen are studied. From the convergence study for the considered physical properties, it has been observed that the coarse mesh reduces the analysis time duration by 4 times approximately than the fine mesh with less than 5% deviation in force-displacement response and hence the coarse mesh is used for further analysis.

Material description

Soft tissue is represented as linear viscoelastic material model and described as in Equation 1 below (PAM-CRASH 2002- solver notes manual 2002, ESI software).

$$G(t) = G_1 + (G_0 - G_1)\, e^{-\beta t} \qquad (1)$$

Where G (t) is the shear relaxation behaviour, G_1 is the long term shear modulus, G_0 is the short term shear modulus and β is the decay constant.

Elastic–plastic material model with steel properties is used to model the top platen. The bottom platen is represented as rigid wall for ease of modelling and faster solution time. Rigid wall representation and elastic plastic model with steel material properties produces similar results, as the deformation in the bottom platen found to be negligible. Initial material properties of soft tissue and top platen are shown in Table 3.

Table 3. Initial material properties of soft tissue and top platen

Soft tissue represented as linear viscoelastic material				
Bulk modulus (K)	Short-term shear modulus (G_0)	Long-term shear modulus (G_1)	Decay constant (β)	Density ρ
Pa	Pa	Pa	s^{-1}	kg/m^3
459200	70120	23370	100	1314
Top platen represented as elastic-plastic material				
Shear modulus	Yield stress	Tangent modulus	Bulk modulus	Density
Pa	Pa	Pa	s^{-1}	kg/m^3
8.08E+10	2.90E+8	8.00E+7	1.75E+11	7820

Contact definition and boundary conditions

Contact interface is defined between the tissue and the top platen. The rigid wall is constrained for zero displacement in all directions. Due to the usage of PTFE sheets during experiments, friction between the rigid wall (bottom platen) and specimen is considered to be zero. Frictional coefficient of 0.02 is applied between the top platen and specimen (Wu et al. 2004). In the top platen, free movement is allowed in the vertical direction while the lateral movement is constrained. In accordance with the experimental conditions used, the soft tissue is analyzed for three average specimen heights (8.93, 9.8 and 9.19 mm) and impact velocities (1.214, 1.786, 2.407 m/s) to identify the material properties at the respective strain rates (136/s, 183/s. 262/s). Displacement of the tissue is measured at the center node on the top surface of the tissue mesh and the axial force is observed from the rigid wall contact force.

PARAMETER ESTIMATION USING TAGUCHI METHODS

In this study, parameter design of Taguchi method is employed to predict the optimum setting level and response values for the selected design parameters. Noise factors are not considered in this study as the design of experiments is run through the analytical model (computer simulations) and assumed to have no variation in the response for identical settings.

Taguchi method has been used in this study to achieve following objectives

1. To estimate the contribution of individual material property in the employed constitutive law.
2. To establish the optimal fit between experimental and finite element stress-strain response and identify the optimal material properties.

Optimal fit between experiment and finite element stress-strain response is established using the following steps,

1. Selection of constitutive law, which is capable of predicting the stress-strain response of soft tissue.
2. Identification of influential material parameters to be tested.
3. Selection of number of levels/settings for the material parameters.
4. Selection of Orthogonal Array (OA) and assigning the material parameters in the matrix.
5. Performing the simulations and recording the response as per the OA matrix.
6. Calculation of main factor effects and predicting the maximum response settings for next iteration until the optimal fit is reached.

Linear viscoelastic constitutive material model is selected to mimic the soft tissue response (Lizee et al, 1998). ”Bulk modulus”, “short-term shear modulus” and ‘long term shear modulus” are identified as design parameters to study its influence in stress-strain response. Maximum stress has been chosen as response variable to conduct this study (Dar 2002). Each parameter is selected with two levels of settings as listed in the Table A1. Level 1 and Level 2 values are chosen as offset values from the initial reference values. Level 1 represents the lower magnitude and Level 2 represents the higher magnitude of the offset value.

The number of degrees of freedom required for finding out the main factor effects is calculated using the selected number of design parameters, its number of setting levels and the overall mean. With three design parameters considered, each having two settings, the total number of degrees of freedom is found to be 3 x (2-1) + 1 = 3. Therefore a minimum of 3 runs is to be simulated to estimate the main factor effects. Standard L_4 (2^3) orthogonal array is selected and the design parameters are assigned in the matrix. Standard orthogonal array is taken from Bagchi 1993. A total of four runs are performed using PAM-CRASH^{TM} finite element software with two setting levels as specified in the orthogonal array. Maximum stress is observed as response parameter. The average response of the main factors is calculated for each setting level. The sensitivity of the material properties are measured using the estimated main effect which provides overall influence of the respective properties on the stress response.

RESULTS AND DISCUSSIONS

EXPERIMENTS

The strain rate dependency of properties in stress strain response is observed for the strain rates at 136/s and 262/s (Figure 4). At 50 % strain, a stress of 0.046 MPa is measured for the lowest average strain rate at 136/s. This value is comparable with stress 0.02-0.024 MPa reported for the compression rate at 0.0083/s on uterine muscle (Pearsall et al. 1978). A stress of 0.11 MPa for extensor digitorum longus (EDL) and 0.085 MPa for tibialis anterior (TA) at 50 % strain are reported (Best et al. 1994) but the type of loading is tensile in nature. Myres et al. (1998) also reported a stress of 0.6, 0.8 and 0.95 MPa for 1/s; 10/s and 25/s respectively at 40% strain for tensile loading. Although the observed stresses from the present study tends to be lower than the stresses reported for tensile loading it is comparative with the results on compression loading which represents the similar conditions as of present study.

Toe modulus

Toe modulus (E_0) is calculated for the linear-toe portion of the stress-strain curve using a linear regression model. The average (mean $\pm$ standard deviation) toe-modulus of the strain rate 136/s is calculated as 0.105 $\pm$ 0.160 MPa (n=7). For the strain rate 183/s, there is a 28% increase in toe modulus showing the mean (SD) as

0.135 (0.062) MPa. The average (mean ± standard deviation) toe-modulus of the strain rate 262/s is calculated as 1.360± 1.09 MPa (n=7). One-way ANOVA for (P<0.05) indicates the increase in toe modulus with increase in strain rate (P= 0.0051).

Tangent modulus

The tangent modulus (E_1) calculated for the non-linear region shows the dependency of strain rate (P=0.023) in the stress strain response and is less sensitive (effect) as compared with toe modulus. The mean (SD) values of the tangent modulus for strain rates 136/s (n=7), 183/s (n=5) and 262/s (n=7) are 0.331 MPa (0.384), 0.455 MPa (0.333) and 3.75MPa (3.70) respectively.

FE ANALYSIS AND PARAMETER ESTIMATION

Identification of linear viscoelastic material properties has been performed using inverse finite element analysis of impact test. From the initial material properties shown in the Table 3, an orthogonal array is formulated for the different material properties so as to study their sensitivity to the response (Table A2).

Maximum stress at approximately 50% of strain is considered as the response parameter to evaluate the parameter settings. Using the response table (Table A3), sensitivity (Figure A1) and response graphs (Figure A2), the maximum possible settings for harmonizing the experimental and finite element model response are identified. The comparison of stress-strain curve during execution of an orthogonal array is shown in Figure A3.

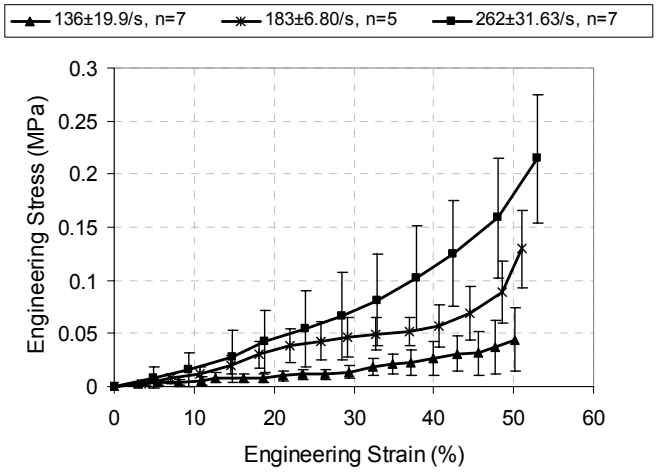

Figure 4. Average stress-strain (mean ± standard deviation) response of 19 specimens tested at strain rates 136/s, 183/s and 262/s

Strain rate 136/s

In this case the bulk modulus as well as the short-term shear modulus shows a larger sensitivity than the long-term shear modulus. The offset range has been taken to be 90 % offset for all the material properties. In this case a decrease in stress is observed with an increase in the long-term shear modulus.

Strain rate 183/s and 262/s

The orthogonal array formulated and the following response for the strain rates 183/s and 262/s are shown in Table A4 to Table A9. The comparison of stress-strain curve during execution of an orthogonal array at first iteration for the respective strain rates are shown from Figure A4 to Figure A7. At a strain rate of 183/s the short-term shear modulus shows a significant influence on the maximum stress variation as compared to the bulk modulus and the long-term shear modulus. At 262/s, all the three material properties show significant influence on stress magnitude for the selected range.

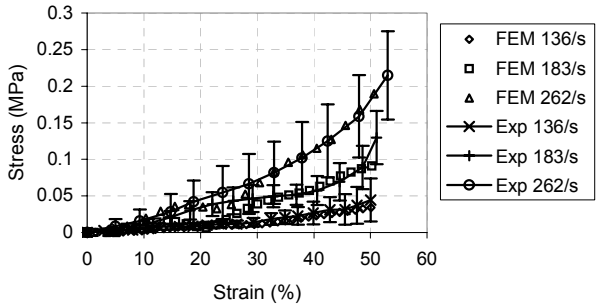

Figure 5. Optimal fit of finite element and experimental stress strain response

The final stress-strain curves obtained from the optimized finite element models are compared with the experimental data. A very good match can be seen in Figure 5. This establishes that this Taguchi method based approach, gives a good estimate of the constants of the material model. The response of finite element simulations at the optimized material properties fits well within the experimental corridor validation of present study (Figure 6).

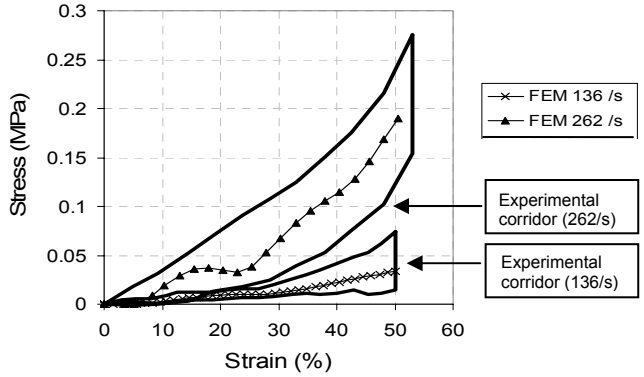

Figure 6. Comparison of finite element stress strain response with identified properties of soft tissue against experimental corridors

The identified material properties of soft tissues for the validated finite element model are shown in the Table 4. The linear viscoelastic material properties extracted at strain rate 183/s and 262/s is compared with Lizee et al. (1998) properties for unknown strain rate as indicated in Table 4. Lizee et al 1998 properties are reported for unknown strain rate and hence the minimum deviation in properties between the studies is expected.

Table 4. Identified material properties for impact-compression loading of soft tissues at different strain rates ranging from 136/s to 262/s

Average Strain rate	Bulk modulus (K)	Short-term shear modulus (G_0)	Long-term shear modulus (G_1)
S-1	Pa	Pa	Pa
136	60614	9256	1893
183	285163	20194	18509
262	353584	53992	14723
Lizee et al. (1998)	250000	115000	86000

The deviation in the identified properties at different strain rates also suspects the validity of the model chosen. Linear viscoelastic model with single properties may not be capable of predicting the response of muscle tissue when impacted at different velocities, as it does not show the strain dependency of material for higher strain rates.

CONCLUSION

An experimental procedure, analytical methods and special instrumentation have been established to measure human soft tissue properties during impact loading at high strain rates. The study has currently been done for strain rates ranging from 136/s to 262/s. Variation of stress-strain behaviour with varying strain rates have been studied. Toe modulus and tangent modulus shows significant strain rate dependency for 50% of strain magnitude as an indication of validity for the experimental procedure adopted. A procedure to map the experimental data from tests over a range of strain rates and strain magnitude to a form that can be useful for finite element simulations using Taguchi methods has been established. Material properties at the optimal fit between finite element and experiment response at the above mentioned strain rates are presented.

FURTHER IMPROVEMENTS AND LIMITATIONS

In the present study the impact direction has been kept perpendicular to the fiber orientation in anterior-posterior direction. The influence of fiber direction on the material properties and the corresponding corridors can be considered as extension of this study. The room temperature has been around 20 deg. C but the tests have not been done under a controlled temperature environment. In this study, a numerical procedure based on repeated FE runs and Taguchi method has been established. Ideally, a method of analytically deducing the characteristics from tests data would have been preferred. The study has currently been done for strain rates between 136 and 262/s, but can easily be (and is being) extended to higher strain rates. Once the variations in these properties at higher rates is known, a single material law can be defined which will incorporate the strain rate effects. A least square fit of experimental and finite element stress-strain response would have been better comparative variable than the maximum stress at 50% strain in error evaluation. Variations in the properties with respect to tissue region, age and other parameters are also a subject of future study.

ACKNOWLEDGMENTS

The authors would like to acknowledge the Department of Science and Technology of India and the support from the Volvo Research Foundation for funding the study. The first author would like to thank Sona Koyo Steering Systems Limited for their support. The authors are also thankful to Mr. Anurag Soni, Mr. Marathe Ratnakar, Mr. Ajay Srivastava and Mr. Rajat from Indian Institute of Technology Delhi, for their help during testing and data processing.

REFERENCES

1. Bagchi, T. P., 1993. Taguchi Methods Explained Practical Steps to Robust Design, Prentice-Hall of India Private Limited, New Delhi.
2. Best, T. M., McElhaney, J., William, E. G., Myres, B. S., 1994. Characterization of the passive response of live skeletal muscle using the quasi-linear theory of viscoelasticity, Journal of Biomechanics, 27, pp. 413-419.
3. Bosboom E. M. H., Hesselink, M. K. C., Oomens, C. W. J., Bouten, C. V. C., Drost, M. R., Baaijens, F. P. T., 2001. Passive transverse mechanical properties of skeletal muscle under in vivo compression, Journal of Biomechanics, 34, pp. 1365-1368.
4. Dar, F. H., Meakin, J. R., Aspden, R. M., 2002. Statistical methods in finite element analysis, Journal of biomechanics, 35, pp. 1155-1161.
5. Delalleau, A., Josse, G, Lagarde, J., Zahouani, H., Bergheau, J. M., 2005. Characterization of the mechanical properties of skin by inverse analysis combined with the indentation test, Journal of Biomechanics, Article in press.
6. Durand-Reville, M., Tiller, Y., Paccini, A., Lefloch, A, Delotte, J., Bongain, A., Chenot, J. L., 2004. Immediate post-operative procedure for identification of the rheological parameters of biological soft

tissue, International Congress Series, 1268, pp. 407-412.
7. Erdemir, A., Viveiros. M. L., Ulbrecht, J. S., Cavanagh, P.R., 2005. An inverse finite-element model of heel-pad indentation, Journal of Biomechanics, Article in press.
8. Iwamoto, M., Omuri, K., Kimapara, H., Nakahaira, Y., Tamura, A., Watanabe, I., Miki, K., 2003. Recent Advances in THUMS: development of individual internal organs, brain, small female and pedestrian model. Proceedings of 4th European LS Dyna Users conference, C:I, pp. 01-10.
9. Karthikeyan, B., Mukherjee, S., Chawla. A., 2005. Characterization of soft tissue under impact loading, Proceedings of JSAE Annual Congress, Paper No. 20055449, 47:5, 5-8.
10. Kauer, M., Vuskovic, V., Dual, J., Szekely, G., Bajka, M., 2002. Inverse finite element characterization of soft tissues, Medical Image Analysis, 6, pp. 275-287.
11. Lizee, E., Robin, S., Song, E., Bertholan, N., Lecoz, J. Y., Besnault, B., Lavaste F., 1998. Development of 3D Finite Element Model of the Human Body. SAE Transactions, Paper No. SAE983152, pp. 2760-2782.
12. Maeno, T., Hasewaga, J., 2001. Development of a finite element model of the total human model for safety (THUMS) and application to car-pedestrian impacts. 17th International Technical Conference on the Enhanced Safety of Vehicles, Paper No. 494, pp. 1- 10.
13. Miller, K., Chinzei, K., 1997. Constitutive modelling of brain tissue: experiment and theory, Journal of biomechanics, 30:11/12, pp. 1115-1121.
14. Miller, K., Chinzei, K., Orssengo, Bednarz, P., 2000. Mechanical properties of brain tissue in-vivo: experiment and computer simulation, Journal of Biomechanics, 33, pp. 1369-1376.
15. Miller-Young, J. E., Duncan N. A., Baroud, G., 2002. Material properties of the human calcaneal fat pad in compression: experiment and theory. Journal of Biomechanics, 35, pp.1523-1531.
16. Moulton, M.J., Creswell, L. L. et al., 1995. An inverse approach to determining myocardial material properties. Journal of Biomechanics. 28, 935-948.
17. Myres, B.S, Woolley, C.T., Slotter, T. L., Garrett, W. E., Best, T. M., 1998. The influence of strain rate on the passive and stimulated engineering stress-large strain behavior of the rabbit tibialis anterior muscle, ASME Journal of Biomechanical Engineering, 120, pp.126-132.
18. Ng, H. W., Teo, E. C., Lee, V.S., 2004. Statistical factorial analysis on the material property sensitivity of the mechanical responses of the C4–C6 under compression, anterior and posterior shear, Journal of biomechanics, 37, pp. 771-777.
19. Oshita, F., Omori K., Nakahira Y., Miki K., 2002. Development of a finite element of a human body, Proc. 7th international LS Dyna user's conference, 3, pp. 37-48.
20. PAM-CRASH Manuals, 2000. Pam System International, ESI Group Software Product Company.
21. Pearsall, G. W., Roberts, V. L., 1978. Passive mechanical properties of uterine muscle (myometrium) tested in vitro, Journal of Biomechanics, 11, pp. 167-176.
22. Roy, R. K., 1990. A primer on the Taguchi method, Von Nostrand Reinhold, New York.
23. Wu, J. Z., Dong R, G., Schopper, A, W. 2004. Analysis of effects of friction on the deformation behavior of soft tissues in unconfined compression tests, Journal of Biomechanics, 37, pp.147-155.
24. Van Ee, C.A, Chasse, A.L, Myres, B. S., 2000. Quantifying skeletal muscle properties in cadaveric test specimens: Effect of mechanical loading, postmortem time, and freezer storage, 122, pp.9-14.
25. Van Ee, C.A, Chasse, A.L, Myres, B. S., 1998. The effect of postmortem time and freezer storage on the mechanical properties of skeletal muscle, SAE Transactions, Paper No. SAE983155, pp.2811-2821.

CONTACT

Dr. Anoop Chawla, Associate Professor,

Department of Mechanical Engineering,

Indian Institute of Technology Delhi,

Hauz Khas, New Delhi -110016, India.

Telephone – (91) – 11- 26591058

E-Mail ID: achawla@iitd.ernet.in

APPENDIX A

Table A1. Setting levels for design parameters

Settings	Bulk modulus (K)	Short-term shear modulus (G_0)	Long-term shear modulus (G_1)
	Pa	Pa	Pa
Level 1	45920	7012	2337
Level 2	872480	133228	44403

Table A2. Trial set for 136/s

Trial	K (Pa)	G_0 (Pa)	G_1 (Pa)	Max. Stress (MPa)
1	45920	7012	2337	0.03
2	45920	133228	44403	0.12
3	872480	7012	44403	0.06
4	872480	133228	2337	0.43

Table A3. Response Table for the trial set for 136/s

Trial	Max. Stress (MPa)	K (kPa)		G_0 (kPa)		G_1 (kPa)	
		45.92	872.48	7.01	133.23	2.34	44.40
1	0.03	0.03	-	0.03	-	0.03	-
2	0.12	0.12	-	-	0.12	-	0.12
3	0.06	-	0.06	0.06	-	-	0.06
4	0.43	-	0.43	-	0.43	0.43	-
Total	0.64	0.15	0.49	0.09	0.55	0.46	0.18
Number of data	4	2	2	2	2	2	2
Average	0.16	0.07	0.25	0.05	0.27	0.23	0.09
Estimated Main Effect		-0.17		-0.23		0.14	

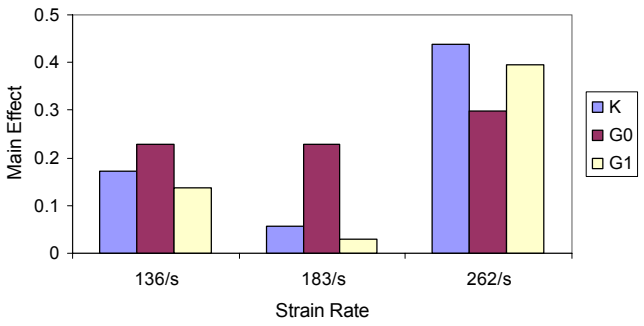

Figure A1. Sensitivity of the material parameters

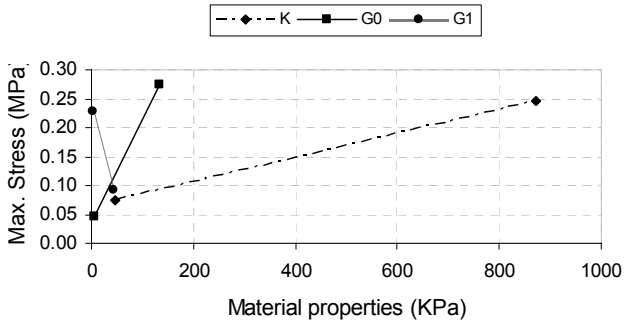

Figure A2. Effect of material parameters on the maximum stress response at a strain rate 136/s

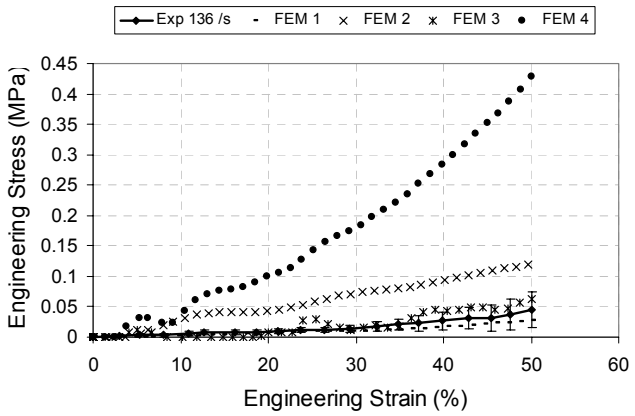

Figure A3. Comparison of experimental data and finite element response for the trial set used for tests at strain rate 136/s

Table A4. Setting levels for design parameters (183/s)

Settings	Bulk modulus (K)	Short-term shear modulus (G_0)	Long-term shear modulus (G_1)
	Pa	Pa	Pa
Level 1	275520	28048	18696
Level 2	642880	112192	28044

Table A5. Trial set for 183/s

Trial	K (Pa)	G_0 (Pa)	G_1 (Pa)	Max. Stress (MPa)
1	275520	28048	18696	0.12
2	275520	112192	28044	0.32
3	642880	28048	28044	0.14
4	642880	112192	18696	0.40

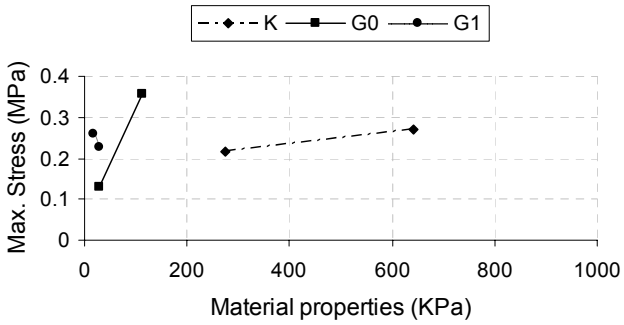

Figure A4. Effect of material parameters on the maximum stress response at a strain rate 183/s

Table A6. Response Table for the trial set for 183/s

Trial	Max. Stress (MPa)	K (kPa)		G_0 (kPa)		G_1 (kPa)	
		275.52	642.88	28.05	112.19	18.70	28.04
1	0.12	0.12	-	0.12	-	0.12	-
2	0.32	0.32	-	-	0.32	-	0.32
3	0.14	-	0.14	0.14	-	-	0.14
4	0.40	-	0.40	-	0.40	0.40	-
Total	0.97	0.43	0.54	0.26	0.72	0.52	0.46
Number of data	4	2	2	2	2	2	2
Average	0.24	0.22	0.27	0.13	0.36	0.26	0.23
Estimated Main Effect		-0.06		-0.23		0.03	

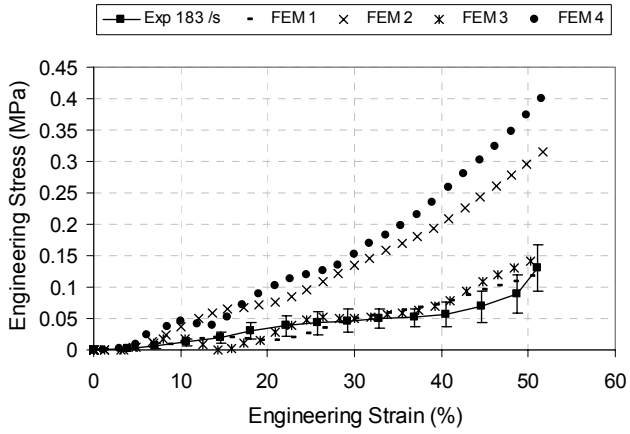

Figure A5. Comparison of experimental data and finite element response for the trial set used for tests at strain rate 183/s

Table A7. Setting levels for design parameters (262/s)

Settings	Bulk modulus (K)	Short-term shear modulus (G_0)	Long-term shear modulus (G_1)
	Pa	Pa	Pa
Level 1	321440	49084	16359
Level 2	596960	91156	30381

Table A8. Trial set for 262/s

Trial	K (Pa)	G_0 (Pa)	G_1 (Pa)	Max. Stress (MPa)
1	321440	49084	16359	0.20
2	321440	91156	30381	0.29
3	596960	49084	30381	1.03
4	596960	91156	16359	0.34

Table A9. Response Table for the trial set for 262/s

Trial	Max. Stress (MPa)	K (kPa)		G_0 (kPa)		G_1 (kPa)	
		321.44	596.96	49.08	91.16	16.36	30.38
1	0.20	0.20	-	0.20	-	0.20	-
2	0.29	0.29	-	-	0.29	-	0.29
3	1.03	-	1.03	1.03	-	-	1.03
4	0.34	-	0.34	-	0.34	0.34	-
Total	1.86	0.49	1.37	1.23	0.63	0.53	1.32
Number of data	4.00	2.00	2.00	2.00	2.00	2.00	2.00
Average	0.46	0.24	0.68	0.61	0.31	0.27	0.66
Estimated Main Effect		-0.44		0.30		-0.39	

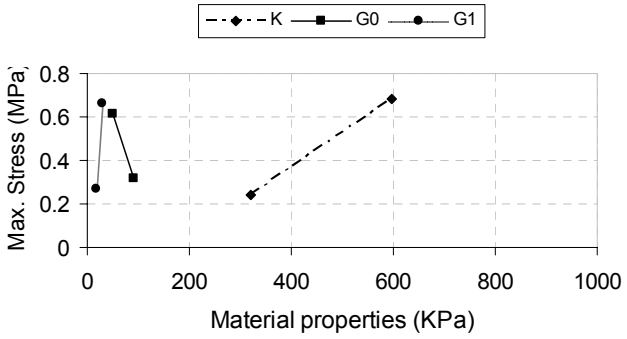

Figure A6. Effect of material parameters on the maximum stress response at a strain rate 262/s

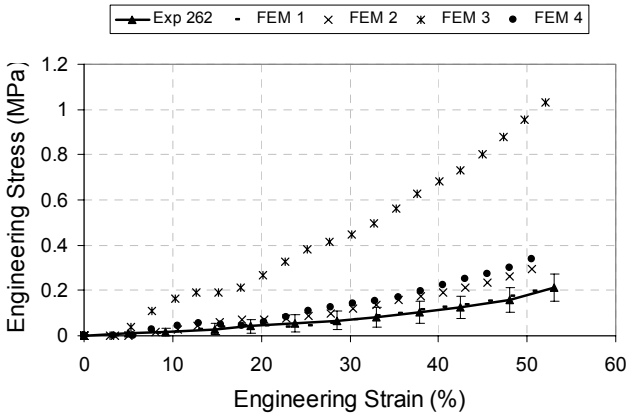

Figure A7. Comparison of experimental data and finite element response for the trial set used for tests at strain rate 262/s